[Frontiers in Bioscience 15, 1007-1017, June 1, 2010]

Photosysem II: where does the light-induced voltage come from?

Mahir D. Mamedov[1], Vasily N. Kurashov[1], Dmitry A. Cherepanov[2], Alexey Yu. Semenov[1]

[1]A.N. Belozersky Institute of Physical-Chemical Biology, Moscow State University, 119991 Moscow, Leninskie gory, [2]A.N. Frumkin Institute of Physical Chemistry and Electrochemistry, Russian Academy of Sciences, Moscow, Russia

TABLE OF CONTENTS

1. ABSTRACT

Photosystem II (PS II) is a biological energy transducer. The enzyme catalyses the light-driven oxidation of water and reduction of plastoquinone. The aim of this work was to review the mechanisms of electrical events in PS II. The major contribution to the total photoelectric response is due to the charge-separation between the primary chlorophyll donor P_{680} and quinone acceptor Q_A accompanied by re-reduction of P_{680}^+ by tyrosine residue Y_Z. The remaining part of the membrane potential is believed to be associated mainly with electron and proton transfer events due to the S-state transitions of the oxygen-evolving complex and proton uptake associated with protonation of the doubly reduced secondary quinone acceptor Q_B. Under certain non-physiological conditions, some other electrogenic reactions are observed, namely: proton-coupled electron transfer between Q_A and non–heme Fe^{3+} and electron transfer from the protein–water interface to the Y_Z radical in the presence of artificial electron donors. These data may provide a good platform for further development of artificial photosynthetic constructs and bio-inspired catalysts.

2. INTRODUCTION

Photosynthesis of green plants, algae and cyanobacteria is the main solar energy converter and provider to the biosphere. During oxygenic photosynthesis energy is captured by linear electron transfer through two pigment–protein complexes, photosystem II (PS II) and photosystem I (PS I), coupled with reduction of CO_2 to sugars in the Calvin cycle. PS II is the first enzyme of the photosynthetic chain in thylakoid membranes. It catalyzes the light-induced oxidation of water to produce molecular oxygen and reduction of plastoquinone to plastohydroquinone (1,2). These reactions are spatially separated and occur on different sides of the reaction center (RC) in the thylakoid membrane.

PS II exists as a large, multisubunit complex with dozens of transmembrane-spanning domains (3,4). The X-ray crystal structure of dimeric PS II core complexes from *Termosynechococcus elongatus* has been recently solved to a resolution of 2.9 Å (5). Each PS II monomer is composed of 20 protein subunits, 25 integral lipids, 35 chlorophyll *a* molecules, 2 pheophytin molecules,

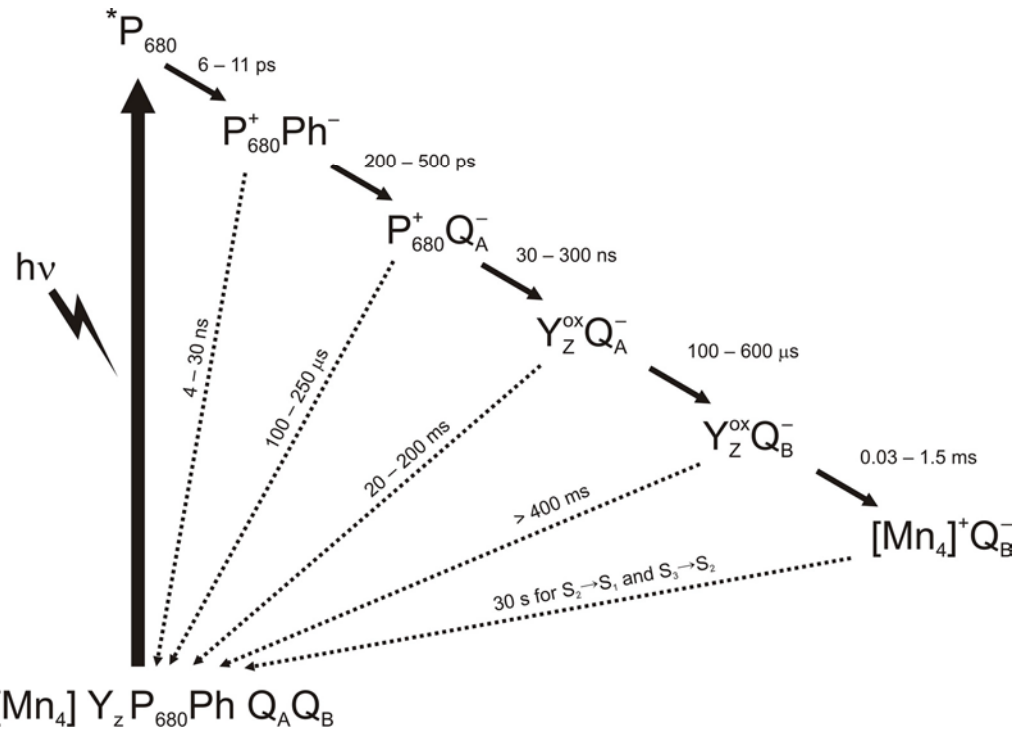

Figure 1. Diagram of the electron transport in PS II along with kinetics of forward and back reactions at room temperature. The recombination reactions (dashed arrows) can occur as true back reactions in a fraction of the centers (redrawn from (7)).

12 carotenoid molecules, 3 plastoquinones (PQ), Mn_4Ca cluster and 1 chloride ion. The minimal photochemically active subsystem of PS II, the RC, contains D1 and D2 proteins, cytochrome b_{559} and the *PsbI* gene product. With the exception of Q_A, all the organic and inorganic cofactors involved in the electron transfer processes are located on the D1 protein of the RC.

A simplified scheme of the kinetics and energetics of electron transfer in PS II is presented in Figure 1. The photochemical events that precede water oxidation are initiated by the capture of light by an antenna complex (CP43 and CP47 kDa) that is located peripherally to PS II RC. The excitation energy is transferred to the photochemically active chlorophyll species P_{680}, triggering a chain of electron transfer reactions across the membrane. Excitation of P_{680} results in formation of the charge-separated state, $P_{680}^{+}Q_A^{-}$, where Q_A is a molecule of plastoquinone. Under physiological conditions, the oxygen-evolving complex (OEC) containing a pentanuclear Mn_4Ca cluster provides electron transfer from water to reduce the cationic radical P_{680}^{+} via a nearby redox-active tyrosine residue Tyr161 of the D1 protein (further denoted as Y_Z), while Q_A^{-} reduces the secondary plastoquinone Q_B. Subsequent charge separations result in further oxidation of the Mn complex. The term 'Mn complex' is used to denote an entity, which comprises the Mn_4Ca core, the ligating amino-acid residues and all water molecules and amino-acid residues, which contribute directly to the elementary steps in dioxygen formation. The oxidation of two water molecules to produce a dioxygen proceeds by storing four oxidizing equivalents by cycling through five so-called S_0-S_4 states, the subscript indicating the number of equivalents stored (6). The states S_0 and S_1 are essentially dark-stable, the states S_2 and S_3 decay within the second-to-minute time range towards the S_1- state.

The secondary quinone, Q_B, functions as a two-electron carrier. Upon receiving two electrons from Q_A and picking up two protons from the medium, Q_B is reduced to hydroquinone form, which binds more weakly to the D1 subunit and is subsequently replaced by an oxidized molecule from the membrane-bound quinone pool.

Thus, PS II couples one-electron charge transfer between Y_Z and Q_A, two-electron/two-proton reduction of the Q_B, and four-electron/four-proton process of water oxidation provided by Mn_4Ca cluster, constituting thereby one of the most sophisticated energy transducers. Flash-induced excitation of RC causes transfer of an electron across the ~35 Å low dielectric profile of the thylakoid membrane. The light-induced voltage ($\Delta\Psi$) originates from the field of the electric dipoles created by the process of charge separation in the photosynthetic RC. The asymmetrical transmembrane organization of RCs makes charge separation reactions electrogenic. $\Delta\Psi$ can be monitored by a variety of methods, namely: microelectrodes, electroluminescence, transient absorbance (electrochromic response of pigments in the light-harvesting complexes), as well as electrometric techniques (see (7) and references therein). The time-resolved measurements of the voltage generated by PS II upon its single-turnover is a valuable tool to obtain information on

the nature and mechanisms of electrogenic reactions and dielectric properties of this pigment–protein complex.

3. ELECTROGENIC REACTIONS INVOLVING PS II TURNOVER

3.1. Early events of light transduction

In photosynthesis, light itself has already done its job within the first time domain (femtoseconds to nanoseconds), and the "light reactions" of photosynthesis are thermodynamically "downhill" electron transfer reactions that are initiated by the much faster events of primary photochemistry (8).

Using the light-gradient technique, which was based on ΔΨ measurements with Ag/AgCl electrodes located at the top and the bottom of the measuring cell, the voltages due to charge separation between P_{680} and pheophytin and further electron transfer resulting in the state $P_{680}^{+}Q_A^{-}$ were demonstrated in pea chloroplasts (9). These stages occur within <50 ps and ~500 ps, respectively, and transfer the electron to the distances equal to 0.58 and 0.42 of the membrane thickness (10). The electrogenic reduction of P_{680}^{+} by the tyrosine Y_Z, which is located at a distance ~7 Å from the closest Mn ion, was demonstrated in PS II membranes oriented in a microcoaxial cell (11).

Note that most of the electrogenic reactions involving PS II turnover within the time range from 200 ns to 100 msec were revealed by the electrometrical technique originally developed in our laboratory (see (12) and references therein). The principle of this method is based on the fusion of photosynthetic vesicles or reconstituted proteoliposomes to a lipid-coated thin collodion film and measurement of ΔΨ in this system using Ag/AgCl macroelectrodes immersed in a buffer electrolyte solution astride the artificial membrane. A slightly different technique makes use of a Teflon film as a support to which a surface of protein–lipid monolayer is absorbed by slowly rising the level of the reservoir (13).

For studying the mechanism of ΔΨ generation due to charge transfer within the complex, some advantages can be gained by the use of the purified PS II complexes, reconstituted in asolectin liposomes. In contrast to thylakoids, this system provides an opportunity to study the effects of exogenous electron donors and acceptors using Mn-depleted and Mn-replenished PS II complexes. The orientation of enzyme in proteoliposomes is highly asymmetric, and the polarity of the electric signals is opposite to that of thylakoids (14). As it was shown by direct electrometrical technique, the relative contribution of ΔΨ component ascribed to $Y_Z \rightarrow P_{680}^{+}$ electron transfer in liposome-reconstituted PS II core particles (~17%) (15, 16) is close to the value obtained by light-gradient method in membrane fragments (~15%) (11). These data indicate that the dielectric permittivity (**ε**) value in this protein region is similar in purified PS II and PS II-enriched membrane fragments. The slower electrogenic phases described in the next sections were normalized to the amplitude of the fast phase due to electron transfer between Y_Z and Q_A.

3.2. Electrogenicity at the donor and acceptor sides of PS II

Many of the catalytic sites of photosynthetic electron transfer are involved in reactions, in which the electron transfer is accompanied by release or uptake of a proton. Based on the redox loop mechanism (17), oxidation reactions on one side of the thylakoid membrane are associated with proton release, whereas reduction reactions on the opposite side of the membrane are due to proton binding.

3.2.1. OEC cycle reactions

The electrogenic reactions associated with electron and proton transfer in thylakoids and in liposome-reconstituted PS II core particles during S-state transitions of the OEC were identified using electrochromic absorption changes of carotenoids (15) and electrometrical technique (15,18). Note that only thylakoids and purified PS II particles are suitable for high time resolution of proton release.

In Figure 2, the properties of the individual S-states and electrogenic reactions at the S-state transitions are schematically indicated. Note that in dark-adapted samples, since almost all the centers are in state S_1 prior to the first flash, possible electrogenic contribution of transition $S_0 \rightarrow S_1$ was neglected. The $S_1 \rightarrow S_2$ transition exclusively involves oxidation of the Mn complex by $Y_Z^{\bullet}$ and it contributes ≤3.5% to the fast $Y_Z^{\bullet}Q_A^{-}$ phase (τ~30-65 μs, pH 6.5) (15). Why this transition lacks an associated deprotonation, remains an open question. Note that the transfer of a proton to the lumenal bulk phase may either occur before or after oxidation of the Mn complex by the Y_Z-radical, but not simultaneously (19). The application of electrometric technique to Mn-depleted PS II (PS II (-Mn)) samples has shown that the electron transfer from exogenously added manganese (4 atoms of Mn per RC) to $Y_Z^{\bullet}$ spans a relative distance of ~5% relative to the distance between Y_Z and Q_A (7). The similar amplitudes of electrogenic reactions due to electron transfer from Mn to Y_Z-radical *in vivo* ($S_1 \rightarrow S_2$ transition) and *in vitro* indicate that the ε value in the protein region between these cofactors remains unchanged during extraction and reconstruction of Mn cluster.

The second photon-induced $S_2 \rightarrow S_3$ transition contributed over 10% to the fast $Y_Z^{\bullet}Q_A^{-}$ phase amplitude (τ ~ 240-300 μs, pH 6.5) both in core particles and in thylakoids. Under these conditions, a proton release precedes an electron transfer from the Mn complex. In so doing, ~7% was ascribed to proton transfer from unidentified amino acid (Arg_{357} of the CP43 protein represents a plausible candidate) in the vicinity of Mn cluster into the lumen and ~3% to electron transfer (15). The first indirect electroluminescence measurements using osmotically swollen chloroplasts showed that transition $S_2 \rightarrow S_3$ was found to be electrogenic and contributed ~5% to the fast phase amplitude (20).

In the $S_3 \rightarrow S_4 \rightarrow S_0$ transition, definitely oxygen and perhaps two protons are released from the Mn

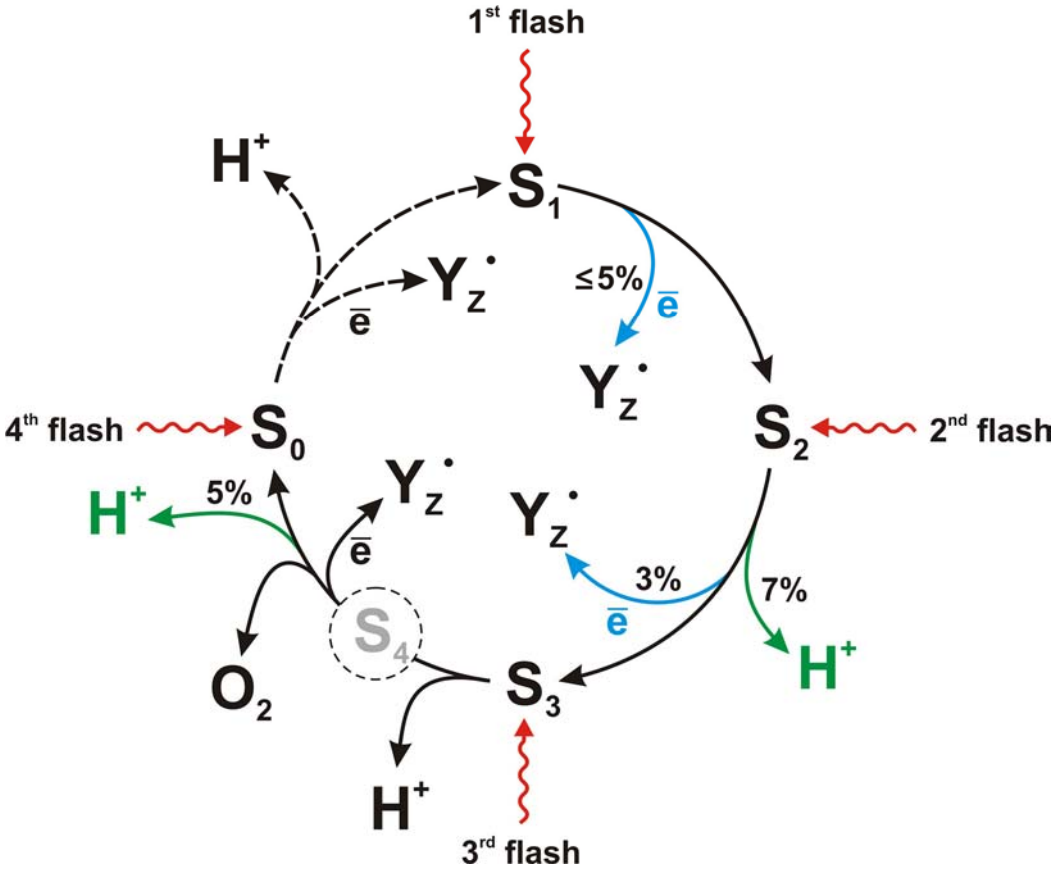

Figure 2. The properties of the individual S-states and electrogenic reactions at the S-state cycle of the oxygen-evolving complex. The S_1-state is prevalent in dark-adapted PS II. Thus, the first flash of light induces the $S_1 \rightarrow S_2$ transition in the majority of PS II. The protons are, most likely, removed from the Mn complex or its ligand environment.

complex. The proton release upon the third photon-induced final oxygen evolving $S_4 \rightarrow S_0$ step revealed relative electrogenic components of ~5% in core particles (pH 6.5) and from ~10% (pH 7.4) to 2% (pH 6.2) in thylakoids (15). The time constants for this transition varied from 1 to 6 ms. Note that S_4-formation does not involve electron transfer from the Mn complex to the Y_Z-radical (formed in <1 μs after light absorption). The central event in the S_4-formation seems to be a deprotonation at the Mn complex induced by $Y_Z^{\bullet}$ (19). In thylakoid membranes, at pH 7.4 the large electrogenicity at final $S_4 \rightarrow S_0$ transient was likely to result from the transfer of protons from bound water into the lumen, while the smallest electrogenicity phase reflected proton transfer to intraprotein bases that were created in the foregoing transitions. It is evident that in dark-adapted samples the extent of proton release as a function of redox transition and pH differs considerably between different samples. In contrast to thylakoids, the absence of any oscillations of proton release in core particles was demonstrated (15). The fourth photon closes the described cycle by promoting the $S_0 \rightarrow S_1$ transition. Under this transition, an electron release (reduction of $Y_Z^{\bullet}$) is followed by the release of a proton. From electrochromic measurements it is clear that no charge is accumulated in the $S_0 \rightarrow S_1$ transition (see (19) and references therein). It has been concluded that this transition may involve oxidation of the Mn complex, as well as charge-compensating deprotonation of the Mn complex or amino acid (s) in the vicinity of the Mn complex.

In contrast to electrogenic reaction $Y_Z \rightarrow P_{680}^+$, the contributions of voltages derived from $S_1 \rightarrow S_2$ and particularly $S_2 \rightarrow S_3$ transitions were less in core particles when compared with thylakoids. It was initially assumed that this difference could be explained by an increase of **ε** around Mn_4 and unidentified amino acid in core particles associated with the absence of 17 and 23 kDa proteins (15). However, the parameters of the electrogenic reactions of the OEC as measured in PS II preparations containing the peripheral proteins of 23 and 17 kD were similar to those of PS II preparations devoid of these proteins. Therefore, it was concluded that neither the 23- nor the 17-kD proteins are involved in the electrogenic reactions of the OEC (18). Clearly, there is still much room for further research.

3.2.2. Y_Z cation reduction by exogenous electron donors

Tyrosine D1-161 (Y_Z) has long been considered as an electron donor for P_{680}^+ in PS II instead of the cytochromes that fulfill this function in bacteria. As mentioned in the Introduction, the photooxidized P_{680} is thought to be reduced by Y_Z, which is, in turn, reduced by an electron from the Mn complex. In native PS II

complexes, $Y_Z^{\bullet}$ is a probable player in the chemical scenario of the abstraction of four electrons and four protons from the two water molecules. It was also demonstrated that the properties of Y_Z in inhibited PS II could be dramatically different from those in active PS II (23,24). It was suggested that Y_Z was located in a hydrophilic environment and exposed to the bulk water in Mn-depleted PS II samples. Several compounds, namely: ascorbate, manganese, *N,N,N'N'*-tetramethyl-*p*-phenylendiamine (TMPD), phenasine metosulfate (PMS), 2,6-dichlorophenol-indophenol (DCPIP), hydroxylamine (NH_2OH), benzidin, 2,5-diphenylcarbazide (DPC) are known to be able to donate electrons to the donor side of PS II RC *in vitro* in the absence of the manganese cluster (see (21) and references therein). *In vivo*, in the absence of active OEC, ascorbate is probably the only alternative electron donor that can supply electrons in sufficiently high amounts to PS II (22).

The addition of a donor capable of donating an electron to the oxidized Y_Z gives rise to competitive substitution of recombination by direct electron transfer in Mn-depleted PS II samples. The data obtained using a direct electrometrical technique showed that the decay kinetics of photoelectric response (the main component of the $\Delta\Psi$ decay kinetics with the lifetime of 20-200 ms) corresponding to the charge recombination between Q_A and $Y_Z^{\bullet}$ slowed down upon increasing the concentration of reduced forms of lipophilic redox mediators, such as TMPD, DCPIP and DPC. At a certain concentration of these substances, the fast generation of the $\Delta\Psi$ related to the electron transfer between Y_Z and Q_A was followed by a new electrogenic phase in the millisecond time domain, which contributed ~17-30% to the fast photoelectric response (21). The effective concentration of DPC was much less than TMPD and DCPIP (50 μM against 1-4 mM). In the presence of DCPIP, the kinetic of the electrogenic phase appeared significantly slower and the amplitude essentially smaller than in the presence of TMPD or DPC. Most probably, the reduced form of the DCPIP is negatively charged at neutral pH, and the existence of a negative charge in the vicinity of either Y_Z or the protein surface at the possible DCPIP binding site may hamper its binding to the protein.

Prior to discussion of the mechanism of PS II electron transfer in the presence of an artificial electron donors, it would be important to note that reduction of laser flash-oxidized primary electron donors (P_{870} in bacterial RC (bRC)) and P_{700} in cyanobacterial PS I complexes) by artificial redox dyes, such as TMPD, DCPIP or PMS, also gives rise to an additional electrogenic phase in the millisecond range (25,26). Because the contribution of an additional electrogenic phase (~20%) to the overall electrogenic response was approximately equal to the contribution of the phase observed in the presence of cytochrome c_2 in the case of bRC (26) and cytochrome c_6 (27) or plastocyanin (28) in PS I, it was concluded that electrogenic reduction of P_{870}^{+}/P_{700}^{+} by redox dyes occured as a result of vectorial electron transfer from the RC protein–water boundary to the protein-embedded Mg-porphyrin rings of P_{870} /P_{700}.

Thus, the data described suggest that the reduction of $Y_Z^{\bullet}$ is not specific for Mn as an electron donor, and the additional voltages registered in the presence of artificial electron donors are due to the vectorial electron transfer from the protein–water boundary to membrane-embedded oxidized tyrosine $Y_Z^{\bullet}$ in Mn-depleted PS II complexes. The data recently obtained in the presence of synthetic trinuclear Mn-complex is also in favor of the latter assumption (29). The electrogenic phase (~25% of the fast phase, τ~160 ms) observed under these conditions was ascribed to the transfer of an electron from the synthetic complex attached to the protein–water interface to the manganese at the protein-embedded Mn-binding site.

Regarding the mechanism of this process, it is important to consider the problem of $Y_Z^{\bullet}$ reduction: direct or through the intermediary pool. Electron tunneling is rapid at short distances, but becomes physiologically too slow well before 20 Å (30). The aromatic amino acids commonly positioned in the protein between the donor and acceptor would enhance electronic coupling and speed up tunneling.

In order to explain the nature of electrogenic phase observed in the presence of exogenous artificial donors, such as DPC or TMPD, we studied the X-ray structure of the donor side of PS II with depleted Mn_4Ca-cluster, which also lacks extrinsic subunits PsbO, PsbU and PsbV. As evident from the structure shown in Figure 3, the removal of these subunits from the PS II structure results in the appearance of the convergent cavity on the donor side of the pigment-protein complex. The floor of the cavity represents the protein site on the protein–water interface that is closest to the tyrosine Y_Z residue. This site has enough space for binding such artificial donors as TMPD or DPC. Figure 3 shows that TMPD molecule rather tightly fits the floor of cavity. The edge-to-edge distance between π-conjugated molecular orbitals of Y_Z and TMPD (oxygen atom of Y_Z and the nearest nitrogen atom of TMPD) is ~17 Å. Taking into account the rate constant of 10^{13} s^{-1} for the electron transfer in the van der Waals contact and the empirical Moser–Dutton rule for the free-energy optimized rate of electron tunneling, this distance corresponds to the rate of ~10^4 s^{-1} (30). This value represents the theoretical upper limit of the rate constant for the 17 Å distance and is about 10 times faster than the observed rate constant of the electrogenic reaction in the presence of saturating concentrations of TMPD and DPC.

Below we show that marked differences exist between NH_2OH and DPC/TMPD/DCPIP in terms of the tyrosine $Y_Z^{\bullet}$ reduction mechanism. It is well known that NH_2OH at micromolar concentrations is an effective electron donor to PS II RC. The slowing down of the photoelectric response decay in the presence of NH_2OH in comparison with the control reflects prevention of charge recombination between Q_A^{-} and $Y_Z^{\bullet}$ by an effective direct electron donation from NH_2OH to RC. The addition of NH_2OH does not lead to appearance of an additional $\Delta\Psi$ rise phase. However, a small component in the $\Delta\Psi$ decay kinetics observed in control sample (characteristic time ~3.5 ms) was slowed down to 25 ms in the presence

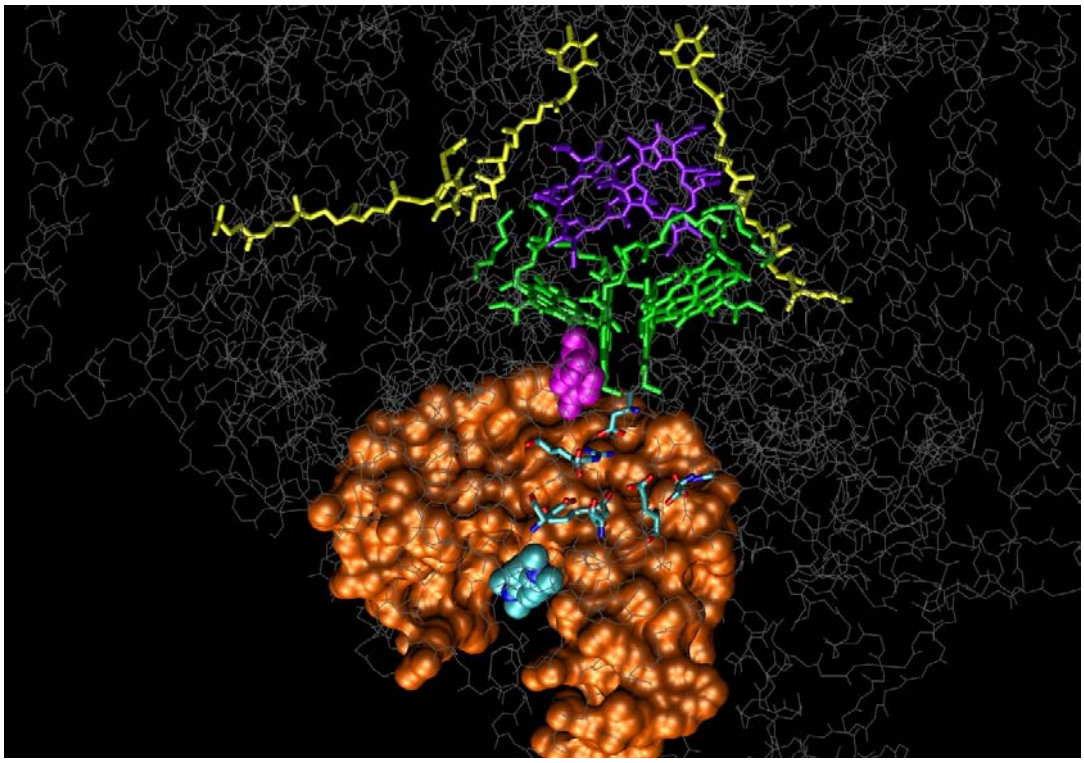

Figure 3. The X-ray structure of the donor site of the Mn-depleted PS II core complexes lacking subunits PsbO, PsbU and PsbV (adopted from PDB enty 3BZ1). Grey lines designate the protein backbone. The protein cavity of the possible TMPD-binding site is shown by orange surface. The position of cavity was found by sampling the smallest distance from tyrosine Y_Z at the protein surface on the donor side of PS II. The carbon atoms of TMPD are marked by cyan and nitrogen atoms by deep blue. The plastoquinone molecules are shown by yellow, pheophytin – by violet, chlorophyll – by green and tyrosine – by magenta. Seven negatively and one positively charged amino acid residues around Mn-depleted cluster are shown by colored sticks.

of NH_2OH. This result can be explained by slowing down of charge recombination in a small fraction of PS II RC as a result of electroneutral electron donation from NH_2OH, or alternatively by the appearance of a small $\Delta\Psi$ rise phase due to electrogenic donation of an electron from NH_2OH binding site to $Y_Z^{\bullet}$ that is compensated by the $\Delta\Psi$ decay phase in the same time scale. It should be noted that a very similar amplitude was reported earlier, but this signal had faster kinetics in the presence of exogenous Mn for PS II (-Mn) samples (29). It can be assumed that the binding site of NH_2OH can be close to the binding site of exogenous Mn.

It is known that some low-molecular compounds, such as NH_3 and close analogue of water, CH_3OH, have at least one common binding site in Mn_4Ca cluster (31). Recently, based on structural and spectroscopic data, it was suggested that methanol binds to the same Mn ion (probably, ^{3}Mn) in all S-states (32). Other group of molecules structurally close to water (H_2O_2, N_2H_4, NH_2OH) are able to reduce the photooxidized Mn-cluster in PS II samples (32). On the basis of the PS II crystal structure, some channels leading from the protein donor side interface to Mn cluster were elucidated (5,33). Three of them have minimal van der Waals diameter of ~2.7 Å. It was suggested that these channels could serve as pathways for the entry of (H_2O) and exit of (O_2).

Extraction of Mn_4Ca cluster also leads to extraction of three peripheral PS II subunits (PsbO, PsbU и PsbV). To elucidate possible channels in this sample, we modeled PS II donor side structure in the absence of these subunits using the program Caver (34). In this structure, three channels with the minimal diameter ~2 Å connecting the Mn_4Ca-binding site and the protein–water interface were revealed. It is obvious that the size of DPC essentially exceeds the diameter of these channels, while the size of NH_2OH molecule allows free diffusion through each of these channels.

The tentative scheme of reduction of photooxidized $Y_Z^{\bullet}$ by DPC and NH_2OH is presented in Figure 4. This figure illustrates the electrogenic reduction of $Y_Z^{\bullet}$ by DPC bound to the protein–water interface, and essentially non-electrogenic reduction of $Y_Z^{\bullet}$ by NH_2OH, which is capable of diffusing through one of the channels connecting this interface with Mn_4Ca-binding site with subsequent reduction of $Y_Z^{\bullet}$.

Thus, the data obtained give new useful information about mechanism of membrane potential generation due to charge transfer on the donor side of PS II. The effective reduction of electrically isolated $Y_Z^{\bullet}$ by electron transfer from artificial electron donors in Mn-

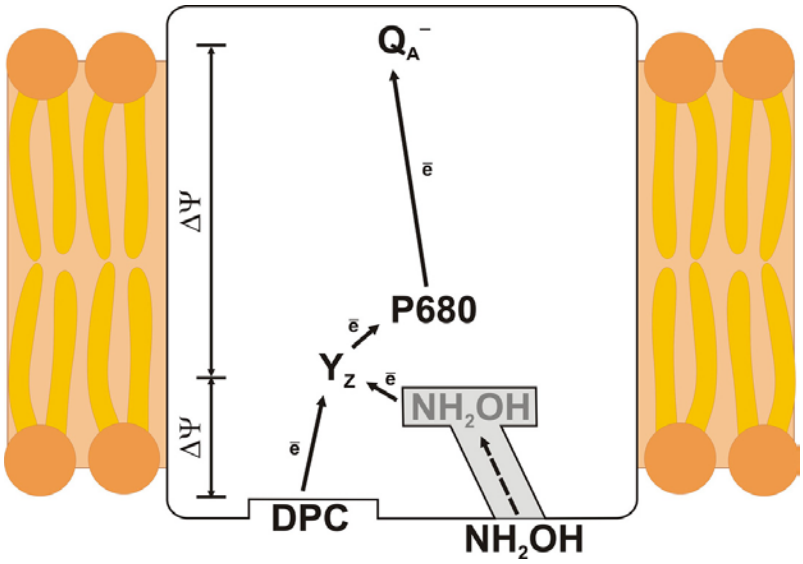

Figure 4. The scheme of electron transport on the donor side of Mn-depleted PS II complexes in the presence of DPC and NH_2OH. Solid arrows indicate electrogenic electron transfer reactions; broken arrow, hypothetical NH_2OH diffusion through one of the hydrophilic channels leading from the protein–water interface to Mn_4Ca-cluster binding site.

depleted PS II complexes can be either electrogenic or electrically silent. More hydrophobic donors (such as DPC, TMPD, DCPIP) reduce $Y_Z^{\bullet}$ electrogenically by vectorial electron transfer from their binding site on the protein–water interface, while more hydrophilic, low-molecular donors (such as NH_2OH) can diffuse through channels with minimal diameter of 2.0 Å, leading from the lumenal protein interface to Mn_4Ca binding site with subsequent reduction of $Y_Z^{\bullet}$. Since dielectrically weighted distance between NH_2OH binding site and Y_Z is not precisely determined, electron transfer from NH_2OH to $Y_Z^{\bullet}$ can be either electrically silent, or make a minor contribution to the overall electrogenesis in comparison with hydrophobic donors. It is likely that the mechanism of $Y_Z^{\bullet}$ reduction by other small molecules, such as, H_2O_2 or N_2H_4, may involve the diffusion through these channels. This suggestion can be tested in future experiments and may provoke the study of the mutants with impaired structure of the channels connecting the Mn_4Ca-binding site and the protein–water interface.

3.2.3. The quinone-iron complex

Light energy is transformed into chemical energy in photosynthesis by coupling light-induced electron transfer to proton uptake. There is no obvious conduction chain between Q_A and Q_B similar to that observed between P_{680} and Q_A, and it is not clear which groups are involved in the electron transfer across the ~20 Å center-to-center distance from Q_A to Q_B.

In RC from purple bacteria and in PS II a high-spin, non-heme ferrous ion is located on the stromal side of the protein between Q_A and Q_B, but it does not function in normal electron flow. However, in contrast to the bRC, electron transfer in PS II is more strongly influenced by changes at the non-heme iron site (35). In a six-coordinate Fe^{2+} center, D1 and D2 proteins histidine residues provide four coordination sites, and exogenous bidentate bicarbonate fills the remaining two coordination sites. It is known that the non-heme iron acts as a single electron carrier under oxidizing conditions and Fe^{3+} reduction is associated with proton binding (36). The electrogenicity of electron and proton transfer at the acceptor side of PS II was monitored by electrochromic absorption changes of carotenoids in thylakoids (37) and by direct electrometrical technique in oxygen-evolving PS II-containing proteoliposomes (38). It was shown that in native PS II complexes whose non-heme iron had been chemically preoxidized, the reduction of Fe^{3+} by Q_A^- following the first flash resulted in the appearance of an additional electrogenic phase (~20% of the fast phase, τ ~ 100 μs at pH 7). This phase is associated with the vectorial proton transfer from the external aqueous phase to amino acid residue (s) in the vicinity of the non-heme iron. This assumption was based on the effects of temperature and H_2O substitution by D_2O on the kinetics of the voltage changes in the oxygen-evolving PS II core complexes. It was shown that the rate of the additional electrogenic phase is decreased by about one-half in the presence of D_2O and is reduced with the temperature decrease.

The partial reoxidation of the non-heme iron by charge recombination with initially oxidized chlorophyll, carotenoid, and tyrosine Y_D within PS II indicates that this electron transfer might be important in the photoprotective transfer of oxidative power away from P_{680}^+ and the oxygen-evolving complex in stressed PS II centers (39).

3.2.4. Protonation of the doubly reduced Q_B^{2-}

Many properties of acceptor quinone complexes of PS II are similar to those of RCs from purple bacteria (40). Electron flow within PS II is gated at the secondary quinone Q_B, which is reduced to PQH_2 only following two consecutive photochemical events. The semiquinone Q_B^-

formed after a single charge separation is firmly bound to the Q_B site and decays slowly to the quinone state by back electron flow to the oxidized $S_{2,3}$ states of the OEC. Doubly reduced reduction state of Q_B is formed because interval between flashes is much faster than the back reaction.

An electrometric technique was used to study the effect of plastoquinone-9 (PQ) substitution by decyl-plastoquinone at the Q_B binding site of PS II core complexes on the electrogenic proton transfer kinetics upon Q_B reduction. The lipophylic environment represented by proteoliposomes has several advantages because they can be considered as a good mimicking system for the photosynthetic membrane, in which the relative amounts of enzyme and quinone can be altered easily, in contrast to the isolated thylakoids or membrane fragments.

No essential $\Delta\Psi$, aside from the phase associated with electron transfer between Y_Z and Q_A (fast phase), is generated when the electron is transferred from Q_A to Q_B, since the two plastoquinones are practically equidistant from the membrane surface, as determined by PS II X-ray crystal structure data (3-5). Only following the second flash, when the formation of a doubly-reduced quinone species Q_BH_2 occurs, trapping of two protons takes place and an additional electrogenic phase of a $\Delta\Psi$ with an amplitude corresponding to ~11% of the fast phase (τ~0.85 ms at pH 7.5) is formed (41). The following observations such as the sensitivity of this phase to diuron, an inhibitor of electron transfer between Q_A and Q_B, the flash-number dependence of its amplitude and the decrease of its rise-time and amplitude with decreasing pH indicate that this electrogenic reaction is associated with protonation of Q_B^{2-} (7). The fact that the amplitude of the phase related to proton-coupled electron transfer between Q_A^- and Fe^{3+} is higher than the phase related to protonation of Q_B^{2-} could be explained by different distances between the non-heme iron/Q_B-binding sites and protein–water interface (3).

An electrometric technique was earlier used to investigate the kinetics of Q_B reduction monitored as the electrogenic charge translocation in *R. sphaeroides* chromatophores in which native coenzyme Q_{10} (UQ) was substituted by its synthetic analogue, decylubiquinone (dQ) (42,43). The data obtained showed that the amplitude of the electrogenic phase due to protonation of Q_B^{2-} contributes ~20% to the fast kinetically unresolvable phase due to formation of $P_{870}^+Q_A^-$.

It should be stressed that there is less conservation between the Q_B sites of PS II and bRC than for the Q_A sites. In addition, the proton pathway connecting the Q_B site to the stromal space is considerably different in PS II compared with bRC. The PS II Q_B site is much closer to the surface than in bRC because of the absence of an equivalent to the bRC H subunit.

In contrast to better-known RC of purple bacteria, in the case of the PS II complexes (40), the mechanism of how Q_B obtains protons from bulk is unknown, although two pathways have been suggested: one involves S264 and H252 on D1 polypeptide (44) and the other, D1-E244, D1-H215 and the iron-bound bicarbonate (36). The latter pathway is preferable because of a favorable pK_α gradient and the important role of bicarbonate in the reduction of Q_B (45).

In conclusion, electrometric measurements provide complementary data to proton uptake measurements performed using other techniques and can help to distinguish between proton-transfer reactions within the RC and surface reactions.

4. CONCLUSIONS AND PERSPECTIVES

In this work, the described voltages involving PS II turnover were mainly derived from electrometrical technique, which allows direct real time measurements of the electric charge movements across the phospholipid membrane. All electrogenic reactions were demonstrated independently of each other. It became evident that the major electrogenicity is due to electron transfer in native enzyme between Y_Z and Q_A, while the remaining of the membrane potential is believed to be associated with vectorial proton (s) release and uptake due to S-state cycle of the OEC and protonation of the Q_B^{2-}, respectively.

Under non-physiological conditions, electrogenic reactions due to proton-coupled electron transfer between Q_A^- and non-heme Fe^{3+}, as well as between artificial electron donors and PS II RC complexes, were also identified.

It became evident that the relative amplitudes of electrogenic reactions are different both at the acceptor (in case of reduced and preoxidized non-heme iron) and at the donor (in case of native and Mn-depleted samples) sides of the PS II complex. The reasons for these differences are not clearly understood. The most likely reason can be due to different dielectric properties in the protein domains, across which the charge transfer occurs (12).

The quality of human life depends to a large degree on the availability of energy. It is evident that the well-being of mankind is threatened unless renewable energy resources can be developed in the near future. Biological systems that harvest free energy from light are of major interest for biotechnology. They may serve as prototypes for gadgets harvesting electric free energy directly from solar illumination. In this respect, the pigment–protein complex of PS II is a key component of the most successful solar energy converting machinery on earth. The enzyme uses solar energy to split water into protons, electrons, and oxygen and gives the organisms an abundant source of electrons. The principles of photosynthesis, the fundamental understanding of light-induced single electron transfer have inspired chemists to mimic these reactions in artificial molecular assemblies. Synthetic light-harvesting antennae and light-induced charge separation systems have been demonstrated by several groups. More recently, there has been an increasing effort to mimic PS II by coupling light-driven charge separation to water oxidation, catalyzed by synthetic manganese complexes (46). Construction of biological-

inspired completely abiotic synthetic representations of the PS II protein scaffolding and catalytic OEC site are also underway in some laboratories.

5. ACKLOWLEDGEMENTS

We thank S.K. and C.S. Chamorovsky for critical reading of the manuscript. The work was supported by grants from the Russian Foundation for Basic Research (09-04-01657-a) and from Russian Federal Agency for Science and Innovation (02.512.11.2286).

6. REFERENCES

1. G. Renger and T. Renger: Photosystem II: The machinery of photosynthetic water splitting. *Photosyn Res* 98, 53-80 (2008)

2. J.P. McEvoy and G.W. Brudvig: Water-splitting chemistry of photosystem II. *Chem Rev* 106, 4455–4483 (2006)

3. K.N. Ferreira, T.M. Iverson, K. Maghlaoui, J. Barber and S. Iwata: Architecture of the photosynthetic oxygen-evolving center. *Science* 303, 1831–1838 (2004)

4. B. Loll, J Kern, W. Saenger, A. Zouni and J. Biesiadka: Towards complete cofactor arrangement in the 3.0 Å resolution structure of photosystem II. *Nature* 438, 1040–1044 (2005)

5. A. Guskov, J. Kern, A. Gabdulkhakov, M. Broser, A. Zouni and W. Saenger: Cyanobacterial photosystem II at 2.9-Å resolution and the role of quinones, lipids, channels and chloride. *Nat Struct Mol Biol* 16, 334-42 (2009)

6. B. Kok, B. Forbush and M. McGloin: Cooperation of charges in photosynthetic O_2 evolution. I. A linear four-step mechanism. *Photochem Photobiol* 11, 467-475.

7. A. Semenov, D. Cherepanov and M. Mamedov: Electrogenic reactions and dielectric properties of photosystem II. *Photosyn Res* 98, 121-130 (2008)

8. J.F. Allen: Light, time and microorganism. In: *Microbial response to light and time*, Eds: M.X. Caddick, S. Baumberg, D.A. Hodgson and M.K. Phillips-Jones, Cambridge University Press, 1-31 (1998)

9. H.-W. Trissl, J. Breton, J. Deprez and W. Leibl: Primary electrogenic reactions in photosystem II as probed by the light-gradient method. *Biochim Biophys Acta* 893, 305–319 (1987)

10. H.-W. Trissl and W. Leibl W: Primary charge separation in photosystem II involves two electrogenic steps. *FEBS Lett* 244:85–88 (1989)

11. A. Pokorny, K. Wulf and H.-W. Trissl: An electrogenic reaction associated with the re-reduction of P680 by tyr Z in photosystem II. *Biochim Biophys Acta* 1184, 65-70 (1994)

12. A.Yu. Semenov, M.D. Mamedov and S.K. Chamorovsky: Electrogenic reactions associated with electron transfer in photosystem I. In: *Advances in photosynthesis and respiration series. Photosystem I: the light-driven, platocyanin:ferredoxin oxidoreductase*, Ed: J.H. Golbeck, Springer, Dordrecht, chapter 21, 319-424 (2006)

13. F. Hook and P. Brzezinski: Light-induced voltage changes associated with electron and proton transfer in photosystem II core complexes reconstituted in phospholipid monolayers. *Biophys J* 66, 2066–2072 (1994)

14. P. Pospíšil and H. Dau: Chlorophyll fluorescence transients of Photosystem II membrane particles as a tool for studying photosynthetic oxygen evolution. *Photosyn Res* 65, 41-52 (2000)

15. M. Haumann, A. Mulkidjanian and W. Junge: Electrogenicity of electron and proton transfer at the oxidizing side of photosystem II. *Biochemistry* 36, 9304-9315 (1997)

16. M.D. Mamedov, E.R. Lovyagina, M.I. Verkhovski, A.Yu. Semenov, D.A. Cherepanov and V.P. Shinkarev: Generation of electric potential by photosystem II from thermophilic cyanobacteria. *Biochemistry* (Mosc) 59, 327-341 (1995)

17. D. Richardson and G. Sawers: Structural biology: PMF through the redox loop. *Science* 295, 1842-18430 (2002)

18. M.D. Mamedov, O.E. Beshta, K.N. Gourovskaya, A.A. Mamedova, K.D. Neverov, V.D. Samuilov and A.Yu.:Semenov: Photoelectric responses of oxygen-evolving complexes of photosystem II. *Biochemistry* (Moscow) 64, 504-509 (1999)

19. H. Dau and M. Haumann: The manganese complex of photosystem II in its reaction cycle – Basic framework and possible realization at the atomic level. *Coord Chem Reviewer* 252, 273-295 (2008)

20. M.H. Vos, H.J. van Gorkom and P.J. van Leeuwen: An electroluminescence study of stabilization reactions in the oxygen-evolving complex of photosystem II. *Biochim Biophys Acta* 1056, 27-39 (1991)

21. O.A. Gopta, A.A. Tyunyatkina, V.N. Kurashov, A.Yu. Semenov and M.D. Mamedov: Effect of redox-mediators on the flash-induced membrane potential in Mn-depleted photosystem II core particles. *Europ Biophys J* 37, 1045-1050 (2008)

22. S.Z. Tóth, G. Schansker, G. Garab and R.J. Strasser: Photosynthetic electron transport activity in heat-treated barley leaves: the role of internal alternative electron donors to photosystem II. *Biochim Biophys Acta* 1767, 295-305 (2007)

23. R.J. Debus: Amino acid residues that modulate the properties of tyrosine Y (Z) and the manganese cluster in

the water oxidizing complex of photosystem II. *Biochim Biophys Acta* 1503, 164-186 (2001)

24. C. Zhang: Interaction between tyrozineZ and substrate water in active photosystem II. *Biochim Biophys Acta* 1757, 781-786 (2006)

25. L.A. Drachev, O.P. Kaminskaya, A.A. Konstantinov, E.A. Kotova, M.D. Mamedov, V.D. Samuilov, A.Yu. Semenov and V.P. Skulachev: Effects of electron donors and acceptors on the kinetics of the photoelectric responses in *Rhodospirillum rubrum* and *Rhodopseudomonas sphaeroides* chromatophores. *Biochim Biophys Acta* 848, 137-146 (1986)

26. K.N. Gourovskaya, M.D. Mamedov, I.R. Vassiliev, J.H. Golbeck and A.Yu. Semenov: Electrogenic reduction of the primary electron donor $P700^+$ in photosystem I by redox dyes. *FEBS Lett* 414, 193-196 (1997)

27. M.D. Mamedov, R.M. Gadzhieva, K.N. Gourovskaya, L.A. Drachev, and A.Yu. Semenov: Electrogenicity at the donor/acceptor sides of cyanobacterial photosystem I. *J Bioenerg Biomembr* 28, 517-522 (1997)

28. M.D. Mamedov, A.A. Mamedova, S.K. Chamorovsky and A.Yu. Semenov: Electrogenic reduction of the primary electron donor P700 by plastocyanin in photosystem I complexes. *FEBS Lett* 500, 172-176 (2001)

29. V.N. Kurashov, E.R. Lovyagina, D.Y. Shkolnikov, M.K. Solntsev, M.D. Mamedov and B.K. Semin: Investigation of the low-affinity oxidation site for exogenous electron donors in the Mn-depleted photosystem II complexes. *Biochim Biophys Acta* 1787, 1492-1498 (2009)

30. C.C. Moser and P.L. Dutton: Engineering protein structure for electron transfer function in photosynthetic reaction centers. *Biochim Biophys Acta* 1101, 171-176 (1992)

31. B. Noring, D. Shevela and G. Renger: Effects of methanol on the S_i-state transitions in photosynthetic water-splitting. *Photosynth Res* 98, 251–260 (2008)

32. F.M. Ho and S. Styring: Access channels and methanol binding site to the $CaMn_4$ cluster in photosystem II based on solvent accessibility simulations, with implications for substrate water access. *Biochim Biophys Acta* 1777, 140-153 (2008)

33. J.W. Murray and J. Barber: Structural characteristics of channels and pathways in photosystem II including the identification of an oxygen channel. *J. Struct. Biol*. 159, 228-238 (2007)

34. P. Medek, P. Benes and J. Sochor: Computation of tunnels in protein molecules based on Delaunay triangulation. *Journal of WSCG* 1, 107-114 (2007)

35. N. Cox, L. Jin, A. Jaszewski, P.J. Smith, E. Krausz, A.W. Rutherford and R. Pace: The semiquinone-iron complex of photosystem II: Structural insights from ESR and theoretical simulation; evidence that the native ligand to the non-heme iron is carbonate. *Biophys J* 97: 2024–2033 (2009)

36. B.A. Diner, V. Petrouleas and J.J. Wendoloski: The iron-quinone electron-acceptor complex of photosystem II. *Physiol Plant* 81, 423–436 (1991)

37. M. Haumann, M. Hundelt, W. Drevenstedt and W. Junge. In: Mathis (ed) Photosynthesis: from light to biosphere, Kluwer, Dordrecht, pp. 333-336 (1995)

38. M.D. Mamedov, A.A. Tyunyatkina., S.A. Siletsky and A.Y. Semenov: Voltage changes involving photosystem II quinone-iron complex turnover. *Eur Biophys J* 35, 647-654 (2006)

39. J.P. McEvoy and G.W. Brudvig: Redox reactions of the non-heme iron in photosystem II: An EPR spectroscopic study. *Biochemistry* 47, 13394–13403 (2008)

40. V.P. Shinkarev: Photosystem II: Oxygen evolution and chlorophyll a fluorescence induced by multiple flashes. In: *Chlorophyll fluorescence: a signature of photosynthesis*, Eds: G.C. Papageorgiou and Govindjee, Kluwer Academic Publishers. pp. 197–229 (2004)

41. M.D. Mamedov, A.A. Tyunyatkina and A.Yu. Semenov: Electrogenic protonation of the secondary quinone acceptor Q_B in spinach photosystem II complexes incorporated into lipid vesicles. *Biochemistry (*Moscow) 70, 1639-1645 (2005)

42. L.A. Drachev, M.D. Mamedov, A.Ya. Mulkidjanian, A.Yu. Semenov, V.P. Shinkarev and M.I. Verkhovsky: Electrogenesis associated with proton transfer in the reaction center protein of the purple bacterium *Rhodobacter sphaeroides*. *FEBS Lett* 259, 324-326 (1990)

43. O.A. Gopta, B.A. Bloch, D.A. Cherepanov, A.Y. Mulkidjanian: Temperature dependence of the electrogenic reaction in the Q_B site of the *Rhodobacter sphaeroides* photosynthetic reaction center: the $Q_A^-Q_B \rightarrow Q_AQ_B^-$ transition. *FEBS Lett* 412, 490-494 (1997)

44. H. Ishikita and E.W. Knapp: Control of quinone redox potentials in photosystem II: Electron transfer and photoprotection. *J. Am. Chem. Soc*. 127, 14714–14720 (2005)

45. J.J.S. van Rensen: Role of bicarbonate at the acceptor side of photosystem II. *Photosyn Res* 73, 185–192 (2002)

46. R. Lomoth, A. Magnuson, M. Sjodin, P. Ping Huang P, S. Styring and L. Hammarstrom: Mimicking the electron donor side of photosystem II in artificial photosynthesis. *Photosyn Res* 87, 25-40 (2008)

Key Words: Photosystem II, Reaction Center, Proteoliposomes, Direct Electrometrical Technique, Electrogenic Reactions, Electron Donors, Channels, Protonation, Review

Send correspondence to: Mahir Mamedov, A.N. Belozersky Institute of Physical-Chemical Biology, Moscow State University, 119992 Moscow, Leninskie gory, Tel: 495-9393188, Fax: 495-9393181, E-mail: mamedov@genebee.msu.su

http://www.bioscience.org/current/vol15.htm